Pergamon

0967-0645(95)00011-9

Deep-Sea Research II, Vol. 42, No. 1, pp. 185–201, 1995

0967-0645/95 $9.50+0.00

Estimation of sticking and contact efficiencies in aggregation of phytoplankton: The 1993 SIGMA tank experiment

AZMY S. ACKLEH,* THOMAS G. HALLAM† and HELENE C. MULLER-LANDAU‡

(*Received* 20 *November* 1994; *in revised form* 20 *December* 1994; *accepted* 6 *January* 1995)

Abstract—The coagulation of phytoplankton, a fundamental mechanism for vertical flux in the oceans and a possible predatory escape mechanism, is a function of the density of suspended particles and at least three enigmatic system processes: the encounter rate of the particles; the contact efficiency of various sized particles upon encounter; and the efficiency of sticking upon contact. A variant of a continuous coagulation model, including the second-order aggregation rate representation and data obtained from the 1993 SIGMA tank experiment at Santa Barbara, are used first to estimate 'stickiness', the efficiency of sticking given that a collision occurs. Primary tools are an inverse, least squares methodology, an aggregation model, and an individual growth model for phytoplankton. The model output corresponds well with the data for smaller sized particles (<0.4 mm^3); however, predicted densities for larger particles were less than observed, and the predicted timing of the bloom was earlier than observed. These anomalies led to an investigation of the interacting roles of stickiness, contact efficiency, and nutrient storage in individual cells. The analyses suggest that (i) aggregation is relatively insensitive to the sticking efficiency, and thus it is difficult to estimate stickiness accurately by fitting aggregation data; (ii) contact efficiency appears to be more functionally variable than assumed in traditional representations, and estimating contact efficiency, jointly with the sticking efficiency, generally produces better agreement with the SIGMA experimental size particle data spectrum; (iii) for the SIGMA tank environment, estimates of contact efficiency are dimensionally more closely related to diameter than to the traditional surface area representation; and (iv) stored nutrient reserves may play a fundamental role in governing timing of peak algal bloom and dynamics of aggregates; inclusion of nutrient storage improves estimation of peak bloom, but does not significantly improve prediction of aggregate dynamics in the SIGMA tank experiment.

INTRODUCTION

The importance of aggregates in oceanic plankton community dynamics (Smetack, 1985; Alldredge and Gotschalk, 1988a,b) has been investigated through a myriad of mathematical models (McCave, 1984; O'Melia and Bowman, 1984; Weilenmann *et al.*, 1989; Jackson, 1990; Hill, 1992; Riebesell and Wolf-Gladrow, 1992; Jackson and Lochmann, 1992; Ackleh *et al.*, 1994a) that discuss the interacting roles of biological components and physical processes in coagulation. Oceanic aggregation is assumed to be governed by a

*Center for Research in Scientific Computation, Department of Mathematics, North Carolina State University, Raleigh, NC 27695-8205, U.S.A.

†Department of Mathematics and Graduate Program in Ecology, University of Tennessee, Knoxville, TN 37996-1300, U.S.A.

‡Department of Mathematics, Swarthmore College, Swarthmore, PA 19081-1397, U.S.A.

multitude of processes including the encounter rate of particles, the contact efficiency of particles given encounter, and the efficiency of sticking after contact. Mathematical representations of these processes (Pruppacher and Klett, 1980) have been employed, but the reliability of parameters, such as stickiness (Ali *et al.*, 1984; Kiørboe *et al.*, 1990; Alldredge and McGillivary, 1991) and other sensitive process representations such as contact efficiency (Hill and Nowell, 1990; Jackson, 1990), limits implementation and predictability of models.

Modeling studies generally have focused on aggregation as an important mechanism for vertical flux of algal losses, with rates comparable to those of zooplankton grazing. Because vertical flux and grazing were relatively unimportant in the SIGMA Santa Barbara Tank Experiment (Alldredge *et al.*, 1995), the experiment provides an excellent data base from which estimates of quantities such as stickiness and contact efficiencies in the coagulation model can be found in the absence of significant confounding factors.

Obtaining experimental values for sticking efficiency has proved difficult as little information is currently available on this parameter or its dependence on physical, chemical and biological properties of the cell. Alldredge and McGillivary (1991) observed that flocculated diatoms in the size range from 0.2 to 7.6 mm had a probability up to 0.88 of sticking to each other. Kiørboe *et al.* (1990, 1994) developed a method for estimating the sticking efficiency from experimental data and a modification of the model of Jackson (1990). They concluded that for some phytoplankton species the stickiness efficiency increases when nutrients are depleted. For others, stickiness is almost constant. We focus on estimation of portions of the coagulation kernel, the sticking and contact efficiencies.

For details about the description of the 1993 SIGMA aggregation experiment at Santa Barbara, refer to Alldredge *et al.* (1995). A cylindrical, 1400 liter tank was set in a temperature controlled environmental chamber and was filled with 1150 liters of natural seawater. The abundance and size distribution of aggregates in the tank were obtained by photographing slabs of seawater. Data were converted to equivalent spherical volume starting with particles of 0.000229 mm^3 and binned into consecutive volume bins, each double the volume of the previous bin.

The SIGMA tank was dominated by diatom species. Our first assumption is that the growth of the dominant diatoms (*Chaetoceros* sp., the primary; *Thalassiosira* sp., the secondary) is approximated by the individual diatom model indicated below. Next, it is assumed that coagulation of particles is approximated by the aggregation model given in Ackleh *et al.* (1994a). An inverse methodology is used here to estimate parameters by fitting the output of the mathematical model to data from the tank experiment. Initially, only sticking efficiency is estimated. Then, the fit is improved by simultaneous estimation of stickiness and of a parameter related to the contact efficiency. Because the parameter estimations obtained yield inaccurate early predictions of the timing of the bloom peak, an alternative algal cell model with a nutrient storage component using first order kinetics (Kooijman, 1993) is developed that fits the delay between nutrient depletion and bloom peak better; this model is then used in the estimation of coagulation parameters.

METHODOLOGY: MODEL AND INVERSE PROCEDURE

The model of Ackleh *et al.* (1994a) used as the reference for the inverse method consists of two parts: an individual portion that describes growth of a single cell, and the other describes the change due to reproduction and coagulation in the densities of different-

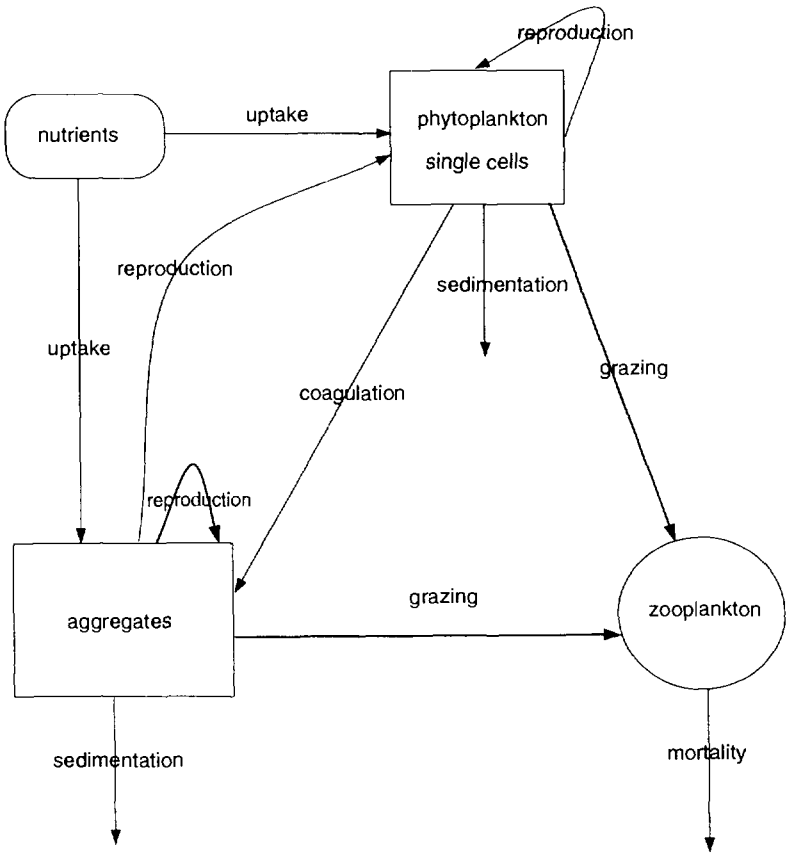

Fig. 1. Conceptual diagram of a plankton community including aggregation. Zooplankton grazing, reproduction in aggregates, and sedimentation are not included in the model analysis presented here.

sized aggregates. Figure 1 presents a conceptual model of the plankton community as impacted by aggregation. The grazing component of the original model in Ackleh *et al.* (1994a) is not utilized here because the zooplankton population density was negligible (Alldredge *et al.*, 1995).

If $C(t)$ is the carbon content of a diatom cell at time t, then the rate of change of carbon with respect to time is the assimilation rate minus the maintenance rate; both physiological process rates are assumed to depend on availability of nutrients. Because organic growth of diatoms occurs within a siliceous frustule (test), cellular uptake is assumed to be proportional to the fixed surface area of the test, with constant of proportionality a (pg μm$^{(-2)}$ day^{-1}). The maintenance costs (respiration rates) are assumed proportional to the cell carbon content with constant of proportionality b (day^{-1}). The individual diatom model is then

$$\frac{dC}{dt} = \frac{N}{k+N}(av^{2/3} - bC) \tag{1}$$

Table 1. Parameter values and units used in the model

Symbol	Interpretation	Value (unit)	Source
v	Volume of cell	1000 (μm^3)	Brzezinski (1985)
x	Volume of aggregate	mm^3	
t	Time	day	
N	Nitrate concentration	μM	
N_0	Initial nitrate concentration	46.3 (μM)	Jackson (1994)
k_N	Half saturation	0.5 (μM)	Scheffer (1991), Jackson and Lochmann (1992)
a	Cell growth rate; no storage	pg μm^{-2} day^{-1}	Calculated
a_s	Cell growth rate; storage	pg μm^{-2} day^{-1}	Calculated
b	Cell maintenance rate; no storage	0.0084 (day^{-1})	Lancelot
b_s	Cell maintenance; storage	1.06×10^{-4} (day^{-1})	Lancelot *et al.* (1991), modified
g	Growth; no storage	1.26×10^{-2}	Calculated from Redfield ratio
g_s	Growth; storage	1.26×10^{-2}	Calculated from Redfield ratio
S_{max}	Maximum density of reserves	9.4×10^{-3}	Fit to C:N experimental data; Alldredge *et al.* (1994)
C_{min}	Initial carbon mass of cell	72.8 (pg)	
$\rho(t, x)$	Density of aggregates	(number mm^{-3} $liter^{-1}$)	Model output
$\alpha(x, y)$	Sticking probability	No dimension	Estimated
$\beta(x, y)$	Coagulation kernel	L $number^{-1}$ t^{-1}	Riebesell and Wolf-Gladrow (1992)

with the initial condition

$$C(0) = C_{min}$$

In equation (1), N is the concentration of the single limiting nutrient, here nitrate (initially, 46.3 μM), k (0.5 μM) is the half-saturation constant for nitrate uptake and v is the fixed volume of the cell siliceous test (μm^3). The maintenance cost per unit carbon in the cell is b (day^{-1}). The surface area related rate of nutrient uptake in carbon equivalents is a (pg mm^{-2} day^{-1}). Table 1 contains the parameter values employed along with their source.

Because of the form of the model, not all parameter values in equation (1) are readily available from the literature; for this reason, reported values of maintenance rate b and volume of the cell are utilized to estimate the value of a from solutions of the model. When nutrients are abundant, then equation (1) can be approximated by the first-order, autonomous model

$$\frac{dC}{dt} = av^{2/3} - bC \tag{2}$$

with initial condition

$$C(0) = C_{min}$$

The exact solution of equation (2) is given by

$$C(t) = \left(C_{min} - \frac{av^{2/3}}{b}\right)e^{-bt} + \frac{av^{2/3}}{b} \tag{3}$$

If the time required for a diatom cell to double its volume and divide under abundant nutrients is $\hat{t}$ (i.e. $C(\hat{t}) = 2C_{min}$), then

$$a = bC_{min}v^{(-2/3)}\frac{(2 - e^{-b\hat{t}})}{(1 - e^{-b\hat{t}})} \tag{4}$$

It is assumed that an individual diatom cell grows according to the model from its minimum initial carbon content C_{min} (μg) until it has doubled in size, at which time the diatom divides into two identical daughter cells. In these simulations the value of $b = 8.4 \times 10^{-3}$ (day^{-1}) was utilized as estimated by Lancelot (1991) for diatoms. The parameter a, the surface area-related rate of nutrient uptake in carbon equivalents (pg mm^{-2} day^{-1}), is calculated using equation (4) and assuming a minimum doubling time ($\hat{t}$) of 0.83 per day (i.e. a maximum growth rate of 1.2 doublings per day). Also the behavior of equation (3) was examined with different b values found in the literature, $b = 0.04$ day^{-1} (EPA, 1985), and b = 0.1 day^{-1} (Jørgensen, 1979) and it was found that the differences in the life history of the model cell (over the range $C_{min} \leq C \leq 2C_{min}$) are negligible among the various choices of b.

When nutrients are depleted, $N = 0$, the model cell enters a resting stage where both growth and maintenance processes effectively cease. Nutrient depletion itself is directly linked to diatom growth and is modeled as

$$\frac{dN}{dt} = -\rho_0(t)g\frac{dC}{dt} \tag{5}$$

where, g (1.26×10^{-2}) is the cost in moles of nitrogen per gram of carbon growth, and $\rho_0(t)$ is the density of single cells at time t. The value of g in this model is directly derived from the Redfield C:N ratio of 106:16 for phytoplankton. Because the C:N ratio changes over time, this is an approximation over the time scale of the experiment. In the computations presented here, cells bound in aggregates neither grow nor reproduce.

The temporal change in the number spectrum or density, $\rho(t,x)$ (numbers mm^{-3} liter^{-1}: also called the number concentration) of aggregates of a given volume x is described by the equation

$$\frac{\partial\rho(t,x)}{\partial t} = F(\rho(t,x)) = \frac{1}{2}\int_0^x \alpha(x-y,y)\beta(x-y,y)\rho(t,x-y)\rho(t,y)\,dy - \rho(t,x)\int_0^A \alpha(x,y)\beta(x,y)\rho(t,y)\,dy \tag{6}$$

where $\beta(x,y)$ represents the rate of collision times the contact efficiency (cm^3 t^{-1} number^{-1}), and $\alpha(x,y)$ is the sticking efficiency (a nondimensional probability). The first term on the right in equation (6) represents the rate at which collisions occur to form new particles with volumes between x and $x + dx$, while the second term expresses the rate at which collisions result in particles being lost from that same size interval.

The rate of collision $\beta(x,y)$, in rectilinear representation, consists of two parts (e.g. Riebesell and Wolf-Gladrow, 1992; Ackleh *et al.*, 1994a). The first, due to shear, has the functional form

$$\beta^s(x,y) = 0.163\left(\frac{\varepsilon}{\nu}\right)^{1/2}(d_x + d_y)^3 EC^s_{x,y} \tag{7}$$

where d_x and d_y represent the diameters of an aggregate of volume x and y, respectively. ε represents the dissipation rate (10^{-6} m^2 s^{-3}), and ν is the kinematic viscosity (1.4×10^{-6} m^{2}sec^{-1}). $EC^s_{x,y}$ is the contact efficiency for shear given by

$$EC^s_{x,y}(d_{min}/d_{max}) = EC_0 \exp\left(-\frac{0.1}{d_{min}/d_{max}}\right) \tag{8}$$

where $d_{min} = \min(d_x, d_y)$, $d_{max} = \max(d_x, d_y)$ and $EC_0 = 1/[\exp(-0.1)]$ (Pruppacher and Klett, 1980). The second part, due to differential settling, has the form

$$\beta^d(x, y) = \frac{\pi(d_x + d_y)^2}{4} |w_x - w_y| EC^d_{x,y} \tag{9}$$

where w_x and w_y are the falling velocities for particles of volume x and y, respectively. The function $EC^d_{x,y}$ is a modified form of the contact efficiency for differential settling given in Pruppacher and Klett (1980)

$$EC^d_{x,y} = \frac{(d_{min}/d_{max})^p}{2(1 + d_{min}/d_{max})^p} \tag{10}$$

Whereas they consider only $p = 2$, here use is made of this more generic form in order to allow the contact efficiency to depend upon relationships other than surface area.

A different construction of $\beta(x, y)$, similar to the curvilinear kernel of Jackson and Lochmann (1993), is

$$\beta^s(x, y) = 1.25\left(\frac{\varepsilon}{\nu}\right)^{1/2} (d_x + d_y)^2 d_{min} EC^s_{x,y} \tag{11}$$

and

$$\beta^d(x, y) = 0.125\pi(d_{min})^2 |w_x - w_y| EC^d_{x,y} \tag{12}$$

As a first step in estimating the sticking efficiency, we assume the traditional value $p = 2$, the rectilinear forms of the coagulation kernels as given in equations (9) and (10), and employ an inverse methodology similar to that developed by Ackleh *et al.* (1994b), based on least square fitting of model output to observed data obtained from the SIGMA tank experiment. To briefly describe the procedure, suppose $N \times M$ observations are given, where M represents the number of different aggregate sizes and N represents the number of times observed. The objective is to minimize, over α, the function

$$J(\alpha) = \sum_{i=1}^{N} \sum_{j=1}^{M} |\log_{10}(\rho(t_i, x_j, \alpha) + 1) - \log_{10}(z_{i,j} + 1)|^2 \tag{13}$$

where $z_{i,j}$ represents the observed densities and $\rho(t_i, x_j, \alpha)$ represents the model output for time t_i and size x_j. The difference in the log of the values is used because the data vary over more than five orders of magnitude, and without this transformation, the function would be biased towards the fitting of the largest values. The case where p is different from 2 is then explored, and the sum of the squares over α and p is minimized.

The spline-based collocation method was used here to solve the model numerically (Ackleh *et al.*, 1994b), and the minimization routine LMDIF obtained from NETLIB library of numerical software to estimate the parameter in question.

Some routine manipulation and a change of integration show that equation (6) conserves volume in that (6) can be written as

$$\int_0^\infty xF(\rho(t,x))\,dx = 0$$

To solve the model equation (6) numerically, the infinite domain of the integral must be truncated; to accomplish this, we replace (6) by

$$\frac{\partial\rho(t,x)}{\partial t} = \frac{1}{2}\int_0^x \alpha(x-y,y)\beta(x-y,y)\rho(t,x-y)\rho(t,y)\,dy - \rho(t,x)\int_0^A \alpha(x,y)\beta(x,y)\rho(t,y)\,dy \tag{14}$$

Equation (14) does not conserve mass unless either α and/or β effectively truncate equation (6). For example, if either of the following are valid (see Ackleh *et al.*, 1994b)

$$\begin{cases}\beta(x,y) \geq 0 \text{ if } x+y \leq A\\ \beta(x,y) = 0 \text{ if } x+y > A\end{cases}$$

or

$$\begin{cases}\alpha(x,y) \geq 0 \text{ if } x+y \leq A\\ \alpha(x,y) = 0 \text{ if } x+y > A\end{cases}$$

then equations (6) and (14) are equivalent. However, because our model parameters do not satisfy these conditions, the numerical methodology is not conservative; some mass is always lost from the system due to formation of aggregates larger than the domain boundaries imposed for simulations.

Because growth in this model occurs only in the presence of nutrients, the bloom is predicted to be at a maximum exactly when nutrients are depleted. Empirical data, however, show a 1–2 day delay between nutrient depletion and bloom peak. To represent growth better, an alternative individual diatom model that included storage of nutrients was constructed. This model follows the same assumptions about nutrient absorption as the previous model, but here the absorbed nutrients are placed first into a storage compartment rather than immediately being incorporated into structural material. Nutrients are then withdrawn from storage and used for growth in proportion to the density, S, of nutrient reserves within the cell (Kooijman, 1993)

$$\frac{dC}{dt} = \frac{S}{S_{max}}\left(\frac{a_s v^{2/3} - b_s C}{g_s + S}\right) \tag{15}$$

$$\frac{dS}{dt} = \frac{a_s v^{2/3}}{C}\left(\frac{N}{k_N + N} - \frac{S}{S_{max}}\right) \tag{16}$$

where S_{max} (9.4×10^{-3}) is the maximum density of nutrient reserves within the cell, and g is, as before, the cost per unit carbon growth in nutrients needed for incorporation into structure. The maintenance constant b_s now has a slightly different interpretation to that of b in equation (1); here it is the cost in nitrogen consumed per unit carbon mass maintained per day, rather than the cost in carbon units. Thus it has a value equivalent to g times its previous value: 1.06×10^{-4}.

The value of S_{max} was chosen to provide a good fit to the C:N ratio observed in the tank when nutrients were abundant and thus in our model, when storage is at a maximum. The data of Alldredge *et al.* (1995) indicate that the minimum ratio of particulate organic carbon to particulate organic nitrogen obtained during the experiment was approximately four. Moreover, this ratio stays at approximately four from Day 2 until Day 10, which coincides with the period of high nutrient abundance. It is assumed that phytoplankton were at their maximum nitrogen storage capacity during this time. In simulations of the individual model, equations (15) and (16), phytoplankton very quickly came to within 5% of their maximum storage capacity whenever ample nutrients were available. At maximum storage, $S = S_{max}$, the total nitrogen in the phytoplankter is the Redfield ratio for nitrogen to carbon in structural material, plus the amount in storage.

It is assumed that the initial storage is close to the maximum storage capacity (specifically, we set $S(0) = 0.9S_{max}$) since at the start of the time period we are fitting, the cells had already been in the nutrient-rich tank for two days.

Because growth is no longer exactly proportional to nutrient depletion, the formulation for nutrient dynamics must be altered to

$$\frac{dN}{dt} = \rho_0(t)\left(-v^{2/3}\frac{N}{k_N + N} + \frac{S}{S_{max}}b_s C\right) \tag{17}$$

The negative term on the right-hand side represents the loss of nutrients from the environment due to uptake by diatoms, while the positive term represents the return of nutrients excreted from the cell during the process of maintenance.

The dynamics of individual cells, as represented by models (1) or [(14) and (15)], are incorporated into the aggregation process by utilizing the first grid point, x_0, in the aggregate size class mesh to represent the single cell population density location. The growth of each single cell is computed by the individual model; the cell divides when the carbon mass reaches $2C_{min}$, with the additional daughter cells added to the number of cells at the mesh point x_0.

Figure 2 presents the data obtained from the SIGMA tank experiment (Alldredge *et al.*, 1995) from Day 2 to Day 14 (but labeled as Day 0 to Day 12 in the subsequent figures) as utilized in our computations as the achievement objective for the model. Because the model output is smoother than the tank data, we interpolate linearly between tank data at computational grid points for purposes of comparison. Because of computational time constraints, the SIGMA tank data is truncated at the size class 1 mm^3, even though the data go from 100 μm^3 to the size class 1000 mm^3. A fixed set of initialization parameters are employed for all of the results reported, including the same initial starting values of $\alpha(0.01)$ and $p(2.0)$. The initial single cell density is a uniform distribution of different sized cells over the interval $[C_{min}, 2C_{min}]$, which has been subdivided into intervals of length $10^{-1}C_{min}$. The initial aggregate densities are set equal to the values measured in the tank at Day 2.

RESULTS

The experimental data as represented in Fig. 2 and model output are compared in two ways, first by employing the mean of the difference of the logarithm of the data and the logarithm of the model output, $\mathcal{M}$,

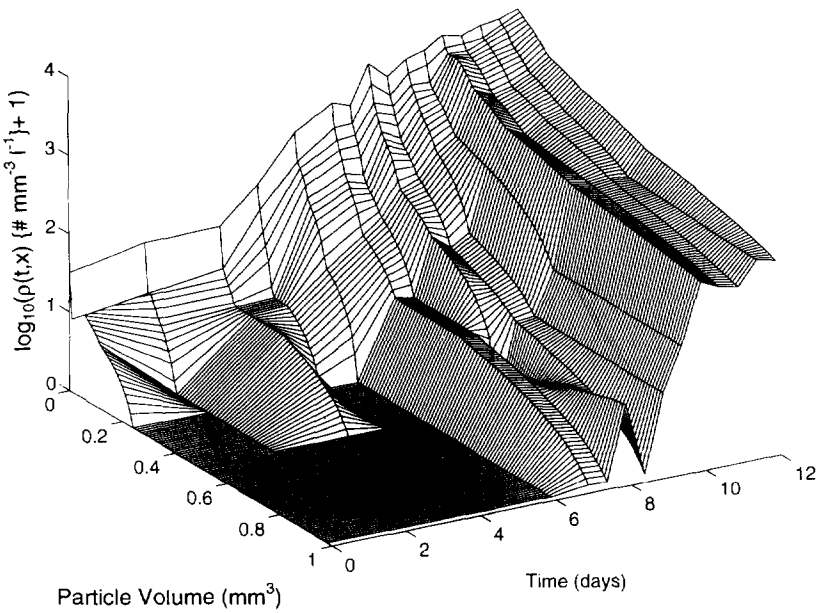

Fig. 2. Graphical representation of observed and interpolated data densities obtained from the Santa Barbara SIGMA tank experiment (Alldredge *et al.*, 1995).

$$\mathcal{M} = \frac{1}{N \times M} \sum_{i=1}^{N} \sum_{j=1}^{M} [\log_{10}(\rho(t_i, x_j) + 1) - \log_{10}(z_{i,j} + 1)]$$

and, second, by using a stronger error estimator, the mean of the difference of the absolute value of the logarithm of the data and the logarithm of the model output, $|\mathcal{M}|$

$$|\mathcal{M}| = \frac{1}{N \times M} \sum_{i=1}^{N} \sum_{j=1}^{M} |\log_{10}(\rho(t_i, x_j) + 1) - \log_{10}(z_{i,j} + 1)|$$

The measure $|\mathcal{M}|$ provides an upper bound on the least square estimator, denoted by $\mathcal{S}^2$, because $\mathcal{S}^2$ is always less than or equal to $|\mathcal{M}|^2$.

In the following computations, the values $N = 16$ and $M = 100$ are used in the estimators.

Assuming the model (1) for diatom growth and the standard surface area related contact efficiency where $p = 2$, a best fit estimation found by the above minimization methodology computes $\alpha = 4.32 \times 10^{-2}$ and the model prediction presented in Fig. 3. This estimation of α yields a model output that agrees well with the data for smaller sized aggregates (size <0.4 mm^3) but yields smaller than observed densities for larger sized aggregates. The mean $\mathcal{M} = 0.25$ (log(number mm^{-3} liter^{-1})), while $|\mathcal{M}| = 0.40$ (log(number mm^{-3} liter^{-1})). The agreement between model results and observations for smaller sized particles and the subsequent deviation for larger particles suggests that the assumed representation for contact efficiency for particles of different sizes might be unsatisfactory, a conjecture proposed by Hill and Nowell (1990). To test this hypothesis, we used the modified form of the contact efficiency for the differential settling by estimating both the power p in the function (9) and α.

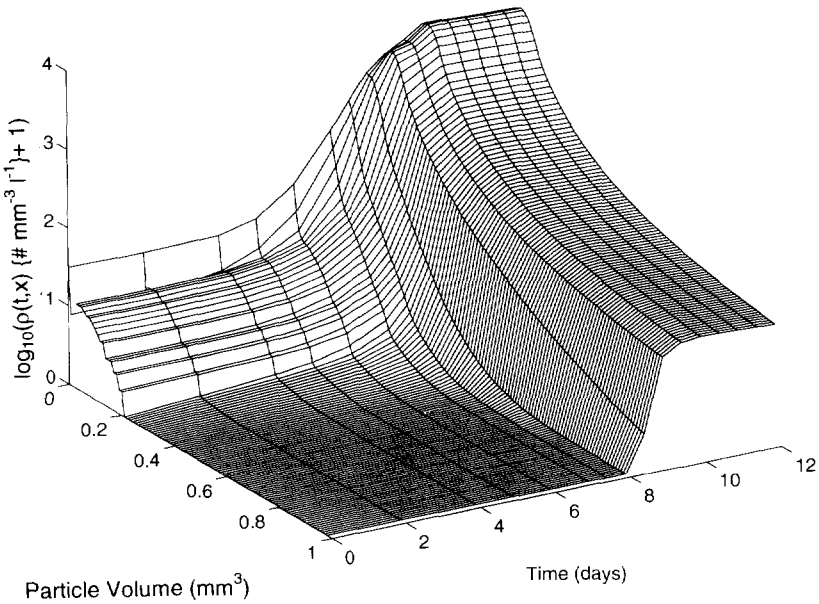

Fig. 3. The aggregation model output densities for the individual model (1) and an estimated value of the stickiness efficiency $\alpha = 4.32 \times 10^{-2}$. In this simulation the theoretical differential settling contact efficiency $EC^{d}_{x,y}$ given in equation (10) was used with $p = 2$.

The inverse methodology can be used to jointly estimate both parameters by minimizing the function

$$J(\alpha, p) = \sum_{i=1}^{N} \sum_{j=1}^{M} |\log_{10}(\rho(t_i, x_j, \alpha, p) + 1) - \log_{10}(z_{i,j} + 1)|^2 \tag{18}$$

The optimization procedure yields estimates of $\alpha = 1.98 \times 10^{-4}$ and $p = 1.33$ (Fig. 4). The agreement of the model with the data is improved for larger aggregates relative to the case where $p = 2$ was assumed and α was estimated but at a cost of a weaker approximation of the smaller size aggregates. The difference between observed data and model output for these particles was computed as $\mathcal{M} = 0.15$ and $|\mathcal{M}| = 0.34$ log(number mm^{-3} liter^{-1}), a slight improvement over the previous computation.

In addition to the above simulation experiments, a time-dependent sticking efficiency was estimated by assuming $p = 2$ and computing α on a daily basis starting from Day 2. From Day 2 to Day 11, the time period where nutrients were available, best fits employing the individual model without storage yield α's larger, generally by two orders of magnitude, than those of simulations from Day 11 to Day 14. This computation agrees with the SIGMA tank experiment (Dam and Drapeau, 1995). On Day 12 of the experiment, growth of phytoplankton essentially ceased and observed densities of aggregates remained stationary, so small sticking efficiencies should be expected.

The peak cell abundance in the model results occurred on Day 11, earlier than the time of the peak of the experiment, Day 12. As stated earlier, one possible explanation of this delay is the presence of a nutrient storage compartment in individual cells, a factor not included in the first individual model. When using the individual model with storage,

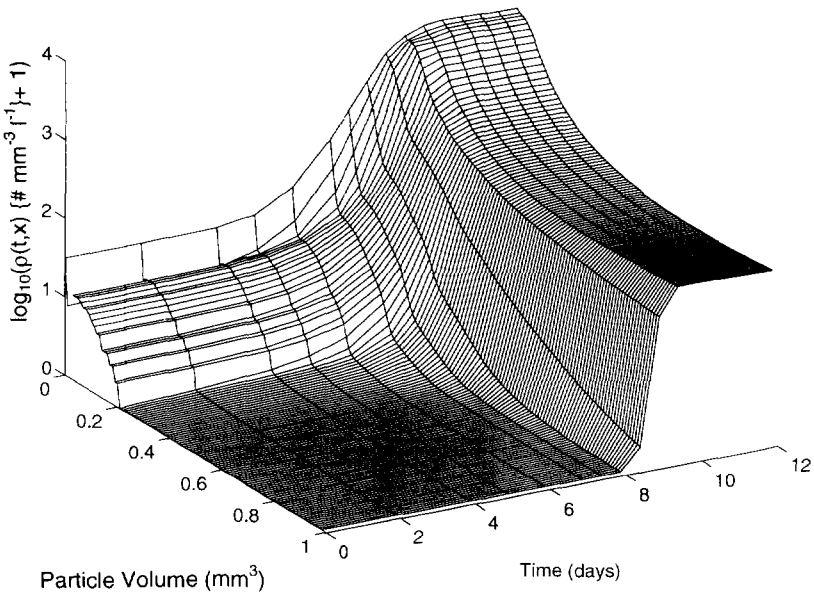

Fig. 4. The aggregation model output densities for the individual model (1) and an estimated value of the power $p = 1.33$ in equation (10) with $\alpha = 1.98 \times 10^{-4}$.

equations (15) and (16), in the aggregation framework, the timing of the peak was predicted to occur at Day 12, a day later than previously. Sensitivity studies on the parameter S_{max} showed that the major effect of increased storage maxima was greater delays between the times of depletion of nutrients and the bloom peaks.

Numerical experiments performed employing the model without storage for the model with storage were repeated. Estimation of α with $p = 2$ yielded $\alpha = 0.37$ with a mean deviation $\mathcal{M} = 0.26$ and $|\mathcal{M}| = 0.40$ log(number mm^{-3} liter^{-1}); see Fig. 5. The optimization procedure to determine both sticking and contact efficiency yields estimates of $\alpha = 1.54 \times 10^{-3}$ and $p = 1.33$ (Fig. 6). The deviations are $\mathcal{M} = 0.16$ and $|\mathcal{M}| = 0.33$ log(number mm^{-3} liter^{-1}).

Sensitivity studies were performed for several critical parameters including doubling time, maximum cell size, and maintenance. The results were somewhat variable, but α was always mobile and p was close to 1.3. Error estimates never deviated much, with a reasonable fit to the data obtained for any reasonable α. The large sensitivity of parameters of the individual model that was observed was due primarily to tight coupling of nutrient and population dynamics. In these experiments, nutrient data from the tank experiment were incorporated directly into the model. Because nutrient dynamics are intricately integrated with the dynamics of the phytoplankton, any deviation from the correspondence between the nutrient uptake and the actual decline in nutrient concentration in the tank data would reflect in the approximation error, making most physiological parameters sensitive. To investigate the sensitivity of the model to nutrient dynamics further, an existing nutrient dynamic model coupled with the aggregation model was employed (Ackleh *et al.*, 1994a) to determine the effect of direct coding of the nutrient data to estimate model parameters. The model production of the nutrient data was

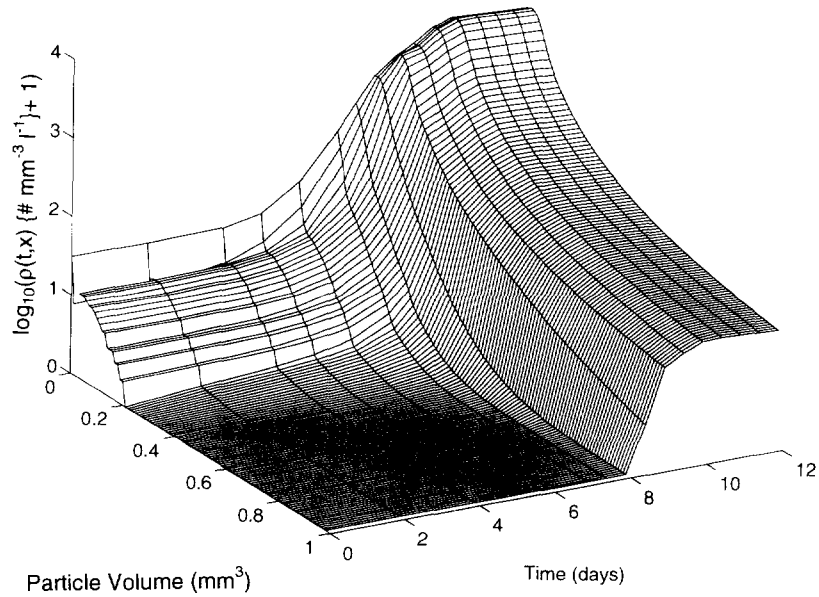

Fig. 5. The aggregation model output densities for an estimated value of the stickiness efficiency $\alpha = 0.37$. In this simulation, the individual model described by equations (15) and (16) was employed and the differential settling contact effieiency $EC^{d}_{x,y}$ given in equation (10) was used with $p = 2$.

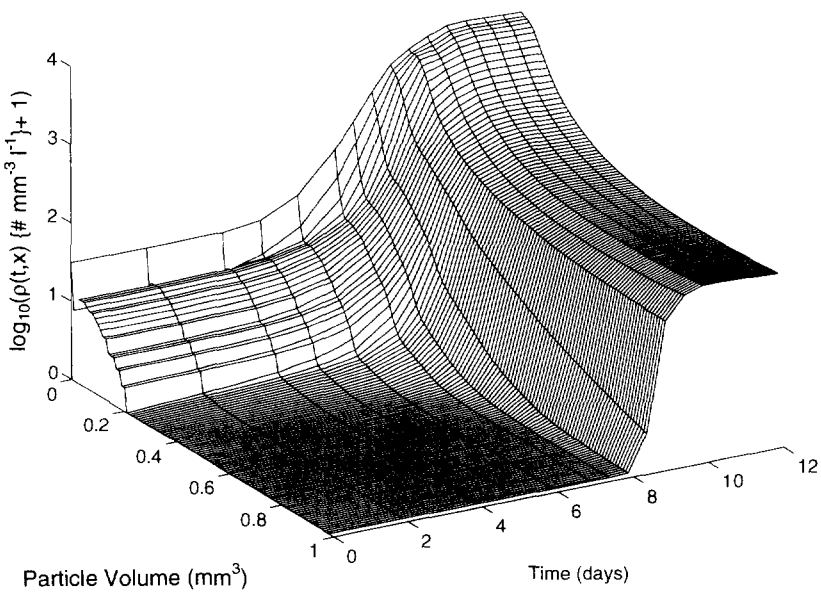

Fig. 6. The aggregation model output densities for the individual model with storage (15) and (16), an estimated value of the power $p = 1.33$ in equation (10) and with $\alpha = 1.54 \times 10^{-3}$.

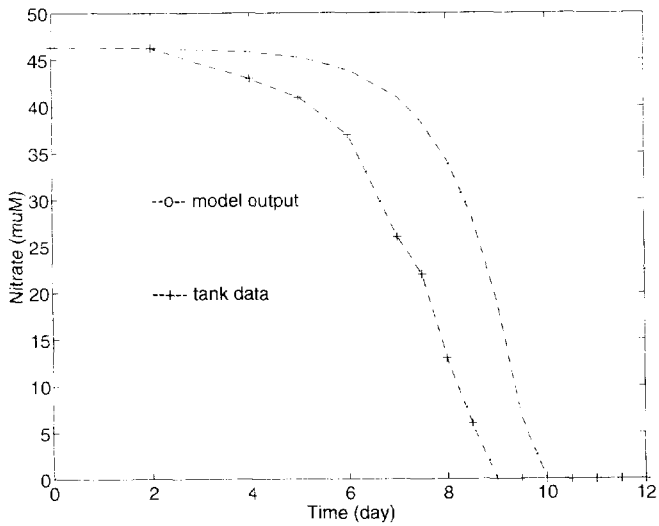

Fig. 7. Observed nutrient dynamics of SIGMA experimental tank (+) and as predicted by nutrient–individual–aggregation model (○). The model nutrient dynamics appear delayed by approximately one day relative to those of the experiment.

advanced by approximately one day as compared to the data (Fig. 7). Had the tank nutrient data not been employed directly in the aggregation model, but rather, our computed nutrient dynamics were used, simulations with the cell model without storage would have reproduced, in error, the bloom peak on the day observed.

The rectilinear coagulation kernel was replaced by the curvilinear coagulation kernel and it was found that production of larger sized aggregates was diminished and the least squares approximation scheme produced significantly larger errors. For example, the curvilinear kernel with $p = 2$ and a least squares estimated value of $\alpha = 10^{-4}$ had $\mathcal{M} = 1.4$ and $|\mathcal{M}| = 1.42 \log(\text{number mm}^{-3}\,\text{liter}^{-1})$. The curvilinear kernel with a jointly estimated $p = 1$ and $\alpha = 1.9 \times 10^{-4}$ yielded $\mathcal{M} = 1.38$ and $|\mathcal{M}| = 1.4 \log(\text{number mm}^{-3}\,\text{liter}^{-1})$; see Fig. 8.

DISCUSSION

To estimate the sticking efficiency parameter a least square fit was used between a model of phytoplankton growth merged into an aggregation representation and the data obtained from the 1993 SIGMA tank experiment at Santa Barbara. This experiment was almost ideal for computational purposes because a comprehensive set of data characterizing nutrient dynamics and aggregate size distributions was obtained. As there was virtually no observed sinking or grazing, losses due to sinking and grazing could be ignored in the model.

Sticking efficiency, an important but elusive parameter in oceanic coagulation processes, thus far has proved difficult to determine in a laboratory, field or numerical experiment. Results here indicate that there may be a fundamental reason for these difficulties. The aggregation process, at least as reflected by the SIGMA tank experiment and by models presented here, is indeed sensitive to changes in stickiness in the model; however, the constraints imposed by the least squares methodology and the large range of values to be fit yield a model environment that is virtually insensitive to sticking efficiency.

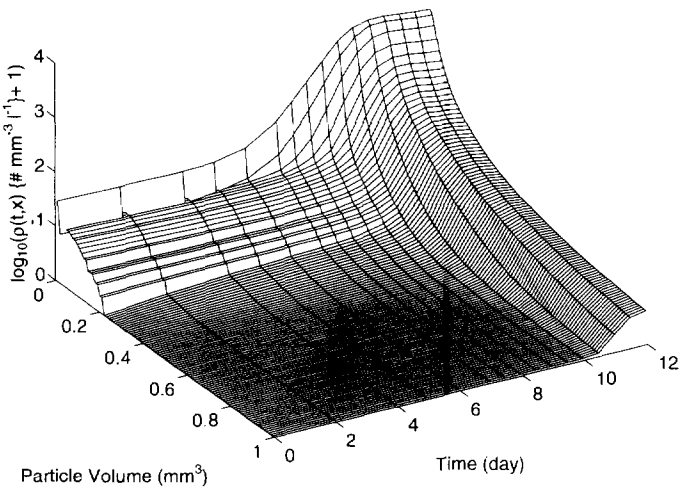

Fig. 8. The model output densities with the cell growth model (1) and the curvilinear kernel given by equations (11) and (12), with least square estimated $p = 1$ and $\alpha = 1.9 \times 10^{-4}$.

Most modeling efforts assume that α is independent of particle size, but other studies (Gibbs, 1983; Alldredge and McGillivary, 1991) report changes in α over size classes. Numerical experiments have showcased some difficulties with traditional approaches to estimate the stickiness efficiency. Using the traditional forms of contact efficiency and estimating sticking efficiency, agreement with the SIGMA experimental data was reasonable but predicted densities for larger particles were always smaller than observed ones. However, in this setting our results are of the same order as those obtained by Dam and Drapeau (1995) who employed a different methodology.

A possible source of these small densities could be utilization of an inappropriate form of contact efficiency. Hill and Nowell (1990) alluded that, in some situations, actual contact efficiencies might be larger than the theoretical ones employed in the aggregation model. The accuracy of contact efficiency representation was considered by modifying the standard form of the contact efficiency for differential settling. The surface area determinant for contact efficiencies for particles of different size, the square power traditionally used in equation (9), was modified to a parameter p that was estimated jointly with α. In this situation, agreement was improved for larger aggregate sizes with an optimal power, approximately $p = 1.3$, obtained in experiments with two quite different individual models, one with storage and one without. This implies that the contact efficiency between a large aggregate of volume $x = 1$ mm^3 and a small one of volume $x = 0.01$ mm^3 is approximately 2/1000, a value closer to the contact efficiencies of $10^{-1} - 10^{-2}$ estimated by Hill and Nowell (1990) than the values obtained from the model when p is set equal to 2. The value of $p = 1.3$ also suggests that contact efficiency is closer to being governed dimensionally by aggregate diameter rather than surface area for the SIGMA tank experiment. This suggested dimension is not physically unreasonable, because the dominant diatoms present in the tank, *Chaetoceros* sp. and *Thalassiosira* sp., are chain-forming algae, where contact should be more a function of length of the chain than surface area. This dimension could also relate to the fact that aggregates are fractals (Logan and Wilkinson, 1990; Kiørboe *et al.*, 1994). The dimension $p = 1.3$ is indicative of the average

fractal dimension associated with the contact between two aggregates, compared with the classical surface area measurement $p = 2$. It is felt that our estimates reinforce implications that classical contact efficiencies may be too small, at least for the SIGMA tank experiment setting, and that methods for improving the estimation of contact efficiencies as well as stickiness should be developed.

The values obtained for the sticking efficiency when $p = 1.3$ are two orders of magnitude lower than when $p = 2$. However, the kernels of the integral in the aggregation equation, the product of the α and β, are of the same approximate magnitude in both instances indicating the tradeoff in the least squares approximation process.

An issue related to modeling methodology unresolved by this approach is the truncation of aggregate size, the subsequent loss of mass conservation, and the consequence that parameter estimation depends upon the truncation. The limiting factor here is that computational power and time requirements increase exponentially as more of the size spectrum is included in the simulations.

Disaggregation is another process that has been omitted in our considerations. Alldredge *et al.* (1995) suggest that aggregates tend to decompose during the final days of the experiment. The model here does not represent this process although this disaggregation process has been discussed in a related, complementary article by Jackson (1995).

The simulations presented here are obtained from a model assumption that cells in aggregates do not reproduce. This assumption is generally invalid, and is particularly so for diatoms and other chain-forming or colony-forming phytoplankton. The lack of reproduction in aggregates may influence parameter estimation in either a positive or a negative manner depending upon other model requirements. For example, our model is adaptable to estimate α with the assumptions that a fixed percentage of cells in aggregates reproduce but the mass of the aggregate remains invariant, so all daughter cells are released to the population as single cells. Unfortunately, theoretical constraints in the present model code do not allow cells to reproduce and a proportion of daughter cells to remain in the aggregate. This process would result in faster transition of smaller aggregates to larger ones which yields higher densities for larger aggregates and could provide densities closer to those observed in the SIGMA experiment. Numerical experiments utilizing larger α values indicate the formation of larger aggregates occurs earlier in the bloom development. For example, for the model without storage, $\alpha = 0.1$, results in significant large-aggregate production on Day 8.

The results presented here are based upon rectilinear coagulation kernels. Curvilinear kernels have been used and some of the simulations have been repeated. Because of a lower density for larger aggregates, the truncation of the size space does not produce as large a loss of mass from the system as the rectilinear kernels. The behavior of the system is similar in that best estimates of contact efficiency still have p closer to diameter than surface area dimension.

The nonlinear phenomena of aggregation and growth drive dynamic time scales in the tank experiment in that an aggregation 'event', a critical numerical level of single cells, must exist for the production of high densities of large aggregates. In the tank, population single cell numbers remain relatively small for the first 8 days, but at Day 10, the number of aggregates increases dramatically as the critical number of single cells is exceeded. The nonlinearity of the aggregation process magnifies this in the production of aggregates, which, in turn, results in lower estimates for α for the later days of the experiment.

From a mathematical perspective, the parameters α and p function differently in the

estimation scheme. Perturbation of α changes the timing of the aggregation 'event' but has little effect on the aggregate densities achieved. A decrease in p allows faster transition of smaller aggregates into larger ones, improving the estimate for the larger aggregates.

This modeling exercise based upon the 1993 SIGMA tank experiment concludes that modeling the processes of coagulation and reproduction of phytoplankton cells enables a good approximation of the observed data, relatively independently of the value of the sticking efficiency. A more fundamental parameter for the experiment is contact efficiency.

Acknowledgements—SIGMA group members, especially Alice Alldredge, Hans Dam, Chris Gotschalk and George Jackson, kindly provided data and important suggestions. Colleen McFadden-Wenig assisted with a portion of the computer code development. The authors would like to thank each of these people as well as Ben Fitzpatrick and two reviewers for helpful comments. This work was supported by the Office of the Naval Research Contract N00014-92-J1139. Research by ASA was also supported by contract AFOSR-F49620-93-0198.

REFERENCES

Ackleh A. S., T. G. Hallam and W. O. Smith (1994a) Influences of aggregation and grazing on phytoplankton dynamics and fluxes. *Nonlinear World*, **1**, 473–492.

Ackleh A. S., B. G. Fitzpatrick and T. G. Hallam (1994b) Approximation and parameter estimation for algal aggregation models. *Mathematical Models and Methods in Applied Sciences*, **4**, 291–311.

Ali W., R. O'Melia and J. K. Edwald (1984) Colloidal stability of particles in lakes: Measurement and significance. *Water Science and Technology*, **17**, 701–712.

Alldredge A. L. and C. C. Gotschalk (1988a) Direct observations of the mass flocculation of diatom blooms: Characteristics, settling velocities and formation of diatom aggregates. *Deep-Sea Research*, **36**, 159–171.

Alldredge A. L. and C. C. Gotschalk (1988b) In-situ settling behavior of marine snow. *Limnology and Oceanography*, **33**, 339–351.

Alldredge A. L., C. Gotschalk, U. Passow and U. Riebesell (1995) Mass aggregation of diatom blooms: Insights from a mesocosm study. *Deep-Sea Research II*, **42**, 9–27.

Alldredge A. L. and P. McGillivary (1991) The attachment probabilities of marine snow and their implications for particle coagulation in the ocean. *Deep-Sea Research*, **38**, 431–443.

Brzezinski M. A. (1985) The Si:C:N ratio of marine diatoms interspecific variability and effects of some environmental variables. *Journal Phycology*, **21**, 347–357.

Dam H. G. and D. T. Drapeau (1995) Coagulation efficiency, organic-matter glues and the dynamics of particles during a phytoplankton bloom in a mesocosm study. *Deep-Sea Research II*, **42**, 111–123.

EPA (1985) *Rates, constants and kinetic formulation in surface water quality modeling*. (Second Edition). EPA/600/3-85/040.

Gibbs R. J. (1983) Coagulation rates of clay materials and natural sediments. *Sedimentary Petrology*, **53**, 1193–1203.

Hill P. S. (1992) Reconciling aggregation theory with observed vertical fluxes following phytoplankton blooms. *Journal of Geophysical Research*, **97**, 2295–2308.

Hill P. S. and A. R. M. Nowell (1990) The potential role of large, fast-sinking particles in clearing nepheloid layers. *Philosophical Transactions of the Royal Society of London*, **331**, 103–117.

Jackson G. (1990) A model of formation of marine algal flocs by physical coagulation processes. *Deep-Sea Research*, **37**, 1197–1211.

Jackson G. (1994) SIGMA Data Report 1. Santa Barbara Tank Experiment, University of California, Santa Barbara, CA.

Jackson G. (1995) Comparing observed changes in particle size spectra with those predicted using coagulation theory. *Deep-Sea Research II*, **42**, 159–184.

Jackson G. and S. Lochmann (1992) Effect of coagulation on nutrient and light limitation of an algal bloom, *Limnology and Oceanography*, **37**, 77–89.

Jackson G. and S. Lochmann (1993) Modeling coagulation of algae in marine ecosystems. In: *Environmental particles*, J. Buffle and H. P. van Leeuwen, editors. Lewis, Ann Arbor, **2**, 387–413.

Jørgensen S. E. (1979) *Handbook of environmental and ecological parameters*. Pergamon Press, London.

Kiørboe T., K. P. Anderson and H. G. Dam (1990) Coagulation effieiency and aggregate formation in marine phytoplankton. *Marine Biology*, **107**, 235–245.

Kiørboe T., C. Lundsgaard. M. Olesen, and J. L. S. Hansen (1994) Aggregation and sedimentation processes during a spring phytoplankton bloom: A field experiment to test coagulation theory. *Journal of Marine Research*, **52**, 297–323.

Kooijman S. A. L. M. (1993) *Dynamic energy budgets in biological systems*. Cambridge University Press, Cambridge, U.K.

Lancelot C. G., G. Billen and H. Barth (1991) The dynamics of *Phaeocystis* blooms in nutrient enriched coastal zones. *Water Pollution Research Report* **23,** *Proceedings of the third workshop held in Plymouth*, U.K., 106 pp.

Logan, B. E. and D. B. Wilkinson (1990) Fractal geometry of marine snow and other biological aggregates. *Limnology and Oceanography*, **35**, 130–136.

McCave I. N. (1984) Size-spectra and aggregation of suspended particles in the deep ocean. *Deep-Sea Research*, **31**, 329–352.

O'Melia C. R. and K. S. Bowman (1984) Origins and effects of coagulation in lakes. *Schweizerische Zeitschrift für Hydrologie*, **46**, 64–85.

Pruppacher H. R. and J. D. Klett (1980) *Microphysics of clouds and precipitation*. Riedel, Boston, 714 pp.

Riebesell, U. and D. A. Wolf-Gladrow (1992) The relationship between physical aggregation of phytoplankton and particle flux: A numerical model. *Deep-Sea Research*, **39**, 1085–1102.

Scheffer M. (1991) Fish and nutrients interplay determines algal biomass: A minimal model. *Oikos*, **62**, 271–282.

Smetack V. S. (1985) Role of sinking in diatom like-history cycles, evolutionary and geological significance. *Marine Biology*, **84**, 239–251.

Weilenmann U., C. R. O'Melia and W. Stumm (1989) Particle transport in lakes: Models and measurements. *Limnology and Oceanography*, **34**, 1–18.